RSC Advances

PAPER

View Article Online
View Journal | View Issue

Cite this: *RSC Adv.*, 2019, **9**, 4162

Quantitative evaluation of relationships between adsorption and partition of atrazine in biochar-amended soils with biochar characteristics†

Zhendong Zhao,[a] Qianqian Wu,[a] Tiantian Nie[a] and Wenjun Zhou *[ab]

Atrazine (ATZ) adsorption in two natural soils amended with biochars produced from different feedstocks at 300, 500, and 700 °C were investigated; further, the relationships between the surface and partition adsorption capacities of ATZ in biochar-amended soils with biochar characteristics were quantitatively evaluated. The results revealed that high aromaticity, hydrophobicity, and low polarity of biochar facilitated ATZ adsorption. The addition of selected biochars significantly increased the adsorption of ATZ on paddy soil (PS) and black soil (BS) by 5.2–7.5 times and 2.3–4.2 times, respectively. On the contrary, the degree of increase in surface adsorption was much higher than that in partition adsorption, mainly due to the role of the specific adsorption of ATZ on biochar. Meanwhile, the respective contributions of surface and partition adsorptions to the total ATZ adsorption on biochar-amended soil changed with different addition amounts of biochar. The multiple nonlinear regression analysis demonstrated the linear dependence of H/C ratio, (O + N)/C ratio, and specific surface area (SSA) of biochar on the surface adsorption capacity of biochar-amended PS and BS, as well as the linear dependence of organic carbon and ash contents on the partition adsorption capacity of biochar-amended PS and the linear dependence of the H/C ratio and SSA on the partition adsorption capacity of biochar-amended BS. In biochar-amended soil systems, interactions between biochar and soil could affect ATZ adsorption, and organic matter in biochar might compensate for the role of soil organic matter in the competition for adsorption sites with a decrease in the biochar pyrolysis temperature.

Received 16th October 2018
Accepted 14th January 2019

DOI: 10.1039/c8ra08544g

rsc.li/rsc-advances

1. Introduction

Biochar is a carbon-rich residue produced by the incomplete pyrolysis of biomass,[1,2] which is widely present in soil and generates potential benefits for carbon sequestration, soil fertility, and immobilization and stabilization of hazardous chemicals,[3–6] due to its distinctive physicochemical characteristics, namely, large specific surface area (SSA), abundant porous structure, multifunctional groups, and strong adsorption capacity.[7–10] Inevitably, these vital characteristics of biochar can be altered once applied to the soil environment *via* short-term or long-term physical, chemical, and biological processes, including natural aging, artificial oxidation, and additional interactions with soil components, such as dissolved organic matter and minerals,[11–14] which, in turn, are likely to affect the adsorption behavior of contaminants, as well as their ultimate transport, fate, and bioavailability in soil.[15]

In particular, studies involving the application of biochar for the immobilization of organic compounds in soil have been extensively reported.[16–19] Biochar exhibited 10–1000 times stronger affinity with organic compounds than natural organic matter; therefore, a small amount of biochar amended into the soil can dominate the overall adsorption of organic compounds.[20] For instance, the addition of only 0.05–0.1% biochar of pine needles to the soil considerably enhanced the adsorption of polycyclic aromatic hydrocarbons.[21] Furthermore, the adsorption behavior of biochar for contaminants was observed to be a function of its physicochemical properties, such as pyrolysis temperature, organic carbon (OC) content, SSA, and pore size distribution. As reported from previous studies, the strong adsorption capacity of biochar in soil could be likely attributed to its high temperature, low OC content, large surface area, and abundant porous structures.[22,23] In addition, it is well known that the addition of biochar into soil not only enhanced the adsorption of organic compounds, but also affected the nature of the adsorption mechanism.[2,24] The increased nonlinear adsorption of organic compounds on biochar-amended soil when compared with that of the original soil suggested the mechanism of transformation from

[a]*Department of Environmental Science, Zhejiang University, Hangzhou, Zhejiang 310058, China. E-mail: wenjunzhou@zju.edu.cn; Fax: +86-571-88982591; Tel: +86-571-88982591*

[b]*Zhejiang Provincial Key Laboratory of Organic Pollution Process and Control, Hangzhou, Zhejiang 310058, China*

† Electronic supplementary information (ESI) available. See DOI: 10.1039/c8ra08544g

a hydrophobic partition in the original soil into the surface adsorption–partition interaction.[25]

Meanwhile, the negative effects of biochar on the adsorption of organic contaminants on biochar-amended soil have also been reported.[26] The interaction between biochar and soil components was considered to be the main factor contributing toward the lower adsorption of organic contaminants by biochar-amended soils. Studies have demonstrated that dissolved organic matter in soil could block the pore surfaces or compete for the adsorption sites of biochar;[19] in addition, soil minerals could exhibit a pore-expanding effect on biochar, which was favorable for the adsorption of organic compounds to the biochar-amended soil than to the original soil.[27] Although studies on the adsorption behavior of organic contaminants on biochar-amended soil have been more frequent, the relationship between the physicochemical characteristics of the added biochar and the adsorption capacity of biochar-amended soil is still not clear. In addition, the mechanisms affecting the adsorption of contaminants on biochar-amended soil have not been fully understood, particularly for the combined surface-partition adsorption mechanism.

In this study, atrazine (ATZ) was selected as the model organic contaminant on behalf of a typical pesticide, due to the long-term utilization of agricultural pesticides and repeated fertilization with animal manure in farmland soil.[23] Biochars derived from rice straw, bamboo, and cow manure were added to two typical agricultural soils in China, namely, paddy soil (PS) and black soil (BS), to examine the effect of biochars produced from different feedstocks on ATZ adsorption by biochar-amended soil *via* a surface-partition adsorption model, and multiple nonlinear regression analysis was used to further reveal the relationship between the surface and partition adsorption capacities of ATZ on biochar-amended soils with biochar characteristics, ultimately providing the theoretical foundation for potential applications of biochar for the remediation of organic contaminants in farmland soils.

2. Materials and methods

2.1 Chemicals and materials

ATZ was purchased from Acros Organics (USA) with a reported purity of 97%, and the detailed molecular structure and physicochemical properties are listed in Table S1.† Rice straw stock was collected from a farmland in the Jiangsu province, China; bamboo stock was purchased from the Zhejiang province, China; cow manure stock was collected from a hoggery in the Anhui province, China. BS and PS were collected from the Heilongjiang and Zhejiang provinces, respectively. HPLC-grade organic solvents used in this study were obtained from Thermo Fisher Scientific Co. Ltd. (USA). All the other reagent-grade chemicals were purchased from Aladdin Chemistry Co. Ltd. (China). Deionized water was used for all the experiments.

2.2 Production and characterization of biochars

Biochars were produced from rice straw, bamboo, and cow manure at a temperature of 300–700 °C, as described by Li *et al.*[27] The detailed method is presented in the ESI.† The obtained biochars were rinsed several times with deionized water to remove the remaining minerals and air-dried, hereafter referred to as RCX, BCX, and MCX, where RC, BC, and MC refer to rice straw biochar, bamboo biochar, and cow manure biochar, respectively, and X refers to the pyrolysis temperature.

The elemental compositions of the biochars were measured using an elemental analyzer (Thermo Finnigan Flash EA 1112), and the ash contents of the samples were determined by heating the sample in a muffle furnace at 800 °C for 6 h. The SSA and pore size distribution of the biochars were determined using the BET N_2 adsorption method. The pH value of the biochars was measured using a pH detector (METTLER TOLEDO S220) with a solid-to-water ratio of 1 : 20 (w/v). The surface functional groups of the biochars were analyzed using Fourier-transform infrared spectroscopy (FTIR). X-ray diffraction (Bruker D8 Advance) was used to determine the crystal mineral formation of biochars from different biomasses.

2.3 Batch adsorption experiments

Batch adsorption experiments were conducted in triplicates according to the guidelines of the Organization for Economic Co-operation and Development (OECD, 2000). A certain amount of BS or PS amended with 0–2.0% (w/w) biochars was weighed into 22 mL glass vials with Teflon-lined screw caps. The ratio was chosen based on the appropriate additive proportion of biochar in natural soils, which guarantees full contact between the biochar and soil in an aqueous suspension. Further, 20 mL of aqueous solutions containing ATZ (0.5–20 mg L^{-1}) was added into each vial. The background solution contained 0.01 M $NaNO_3$ to maintain a constant ionic strength, 100 mg L^{-1} NaN_3 to minimize biodegradation, and solution pH was adjusted by the addition of 0.1 M HNO_3 or NaOH to ensure desirable pH at the adsorption equilibrium.

The preliminary experiments indicated that 48 h was sufficient to attain equilibrium for ATZ adsorption by biochars and soils; further, microbial degradation, volatilization, and adsorption to glass walls were negligible during the adsorption experiments. The glass vials were maintained in dark, shaken for corresponding time at 25 °C, and centrifuged for 10 min. An appropriate aliquot of the supernatant was then filtered through a 0.45 μm nylon membrane.

The ATZ concentration in the supernatant was determined by HPLC (LC-20AT, Shimadzu, Japan) equipped with an Agilent Eclipse XDB-C_{18} reversed-phase column (4.6 × 150 mm, 5 μm, Supelco, USA) and a UV detector at 225 nm at a column temperature of 25 °C. Methanol/water (70 : 30, v/v) was employed as the mobile phase for ATZ. The equilibrium adsorption amount of ATZ was calculated according to the mass difference between the initial and equilibrium concentrations in aqueous solutions.

3. Results and discussion

3.1 Biochar characterization

The physicochemical properties including pH, bulk elemental compositions, ash content, and atomic ratios of biochars

Table 1 Physicochemical properties of RC300–700, BC300–700, and MC300–700

			Elemental composition						
Sample	pH	Ash (%)	C (%)	H (%)	N (%)	O (%)	H/C	O/C	(O + N)/C
RC300	7.19	19.15	54.91	3.04	1.29	21.61	0.66	0.26	0.283
RC400	9.12	23.28	54.96	2.23	1.26	18.27	0.49	0.22	0.241
RC500	10.20	25.19	57.00	1.72	1.08	15.01	0.36	0.18	0.192
RC600	10.20	26.58	61.16	1.09	0.93	10.24	0.21	0.11	0.125
RC700	10.33	27.65	63.35	0.95	1.12	6.93	0.18	0.073	0.088
BC300	6.87	1.38	72.93	3.79	0.58	21.32	0.62	0.20	0.20
BC400	8.12	1.68	77.64	3.28	0.66	16.74	0.51	0.14	0.15
BC500	9.16	2.0	82.41	2.59	0.70	12.3	0.38	0.099	0.11
BC600	10.44	2.24	87.93	1.71	0.78	7.34	0.23	0.056	0.063
BC700	10.37	3.63	89.85	0.94	0.81	5.97	0.13	0.035	0.043
MC300	7.54	34.15	45.74	3.21	2.62	17.28	0.84	0.21	0.26
MC400	8.10	38.38	45.28	2.59	2.28	14.47	0.69	0.17	0.21
MC500	9.04	46.03	42.45	1.49	2.08	11.45	0.42	0.13	0.16
MC600	9.22	48.2	44.32	1.07	2.04	8.14	0.29	0.065	0.11
MC700	9.53	52.63	41.84	0.61	1.21	6.71	0.20	0.059	0.084

produced from different feedstocks at 300–700 °C are listed in Table 1. Under the same pyrolysis temperature, biochar properties were strongly feedstock-dependent. The C contents of biochars derived from bamboo were observed to be far higher than those derived from rice straw and cow manure. By contrast, MC exhibited the highest ash content, followed by RC and BC, which was consistent with previous studies.[25] In this study, ash (or mineral) presence was attributed to the silica for MC and potassium chloride for RC by means of the XRD spectra (Fig. S1†). These properties were comprehensively reported in an earlier study.[28] The calculated H/C, O/C, and (O + N)/C atomic ratios of biochar were used as indexes for aromaticity, hydrophobicity, and polarity, respectively.[29] The higher H/C ratios of MC indicated a lower degree of carbonization and aromaticity when compared with those of RC and BC, while the higher O/C and (O + N)/C ratios of RC suggested the lower hydrophobicity and higher polarity than BC and MC. BC had the lowest polarity among all the studied biochars due to the lower ash content than RC and MC, which could induce an adverse effect on the protection of O-containing functional groups.[30] This was also consistent with the previous conclusion that the deashing treatment of the biochar with high ash content decreased the surface polarity to a large extent. A van Krevelen diagram was used to understand the selective loss of elements during the hydration and carbonization of biochar by comparing the H/C and O/C ratios (Fig. S2†). The decrease in aromaticity of the biochars resulted in a consequent decrease in hydrophobicity, which was ascribed to the loss of volatile hydrocarbons and increase in C contents of the biochars.[31]

The SSA and pore size distribution of all the biochars are listed in Table 2. The SSA and total pore volume (TPV) of the biochars derived from different feedstocks gradually increased with the increase in the pyrolysis temperature. It was clearly obvious that BC had the largest SSA and micropore volume (MPV), particularly at a relatively high temperature; this indicated that BC had a more abundant pore structure than RC and MC. The surface functional groups of biochars were characterized by FTIR, and the corresponding spectra are shown in Fig. S3.† The reduction in the intensity of the peaks at 2931 cm^{-1}, 1370 cm^{-1}, and 1458 cm^{-1} assigned to the stretching vibration of $–CH_2–/–CH_3$ and the increase in the intensity of the peak at 1596 cm^{-1} assigned to the stretching vibration of with an increase in the pyrolysis temperature exhibited the transformation of aliphatic carbons into aromatic carbons. Meanwhile, the attenuation in the intensity of the peak at around 3400 cm^{-1} assigned to the stretching vibration of –OH showed decreased polarity with an increase in the pyrolysis temperature of biochars.

3.2 Structure–activity relationship between biochar physicochemical properties and adsorption capacity for ATZ

The adsorption isotherms of ATZ on RC300–700, BC300–700, and MC300–700 are shown in Fig. S4,† and the Freundlich model fitting parameters are listed in Table S2.† The adsorption data effectively fitted the Freundlich model as indicated by the correlation coefficients ($R^2 \geq 0.96$). The adsorption capacities of the biochars for ATZ increased with the pyrolysis temperature. Among the three types of biochars produced at 300–700 °C, RC showed the highest adsorption affinity toward ATZ. Moreover, the adsorption isotherms of biochar produced at 500–700 °C showed stronger nonlinearity with n values ranging from 0.195 to 0.509, which indicated that pore-filling, H-bonding effect, and π–π electron donor–acceptor (EDA) interaction played a critical role in the adsorption of organic compounds on carbonaceous adsorbents in addition to hydrophobic partition.[30,32] Further, this nonlinearity was found to be more significant for MC than BC and RC.

As reported from previous studies, several possible interactions including hydrophobic effect, H-bonding, π–π EDA, and their strength and contribution to the overall adsorption were a function of the properties of both organic compounds and adsorbents.[33,34] For example, the adsorption of hydrophobic organic contaminants (HOCs) on low-temperature biochars that generally contained more hydrophilic groups could be involved in more interactions *via* specific adsorption including H-bonding and π–π EDA interaction between the aromatic

Table 2 SSA and pore size distribution of RC300–700, BC300–700, and MC300–700

Biochar	[a]SSA ($m^2\ g^{-1}$)	[b]MPA ($m^2\ g^{-1}$)	[c]ESA ($m^2\ g^{-1}$)	[d]TPV ($cm^3\ g^{-1}$)	[e]MPV ($cm^3\ g^{-1}$)	[f]APD (nM)	SSA/OC ($m^2\ g^{-1}$)
RC300	7.981	0.000	18.645	2.06×10^{-2}	0.000	10.351	14.532
RC400	13.562	0.000	17.566	2.12×10^{-2}	0.000	6.275	24.674
RC500	22.445	16.692	13.727	2.84×10^{-2}	0.015	4.621	39.375
RC600	106.163	89.301	23.441	9.52×10^{-2}	0.073	3.382	173.575
RC700	141.124	102.772	29.728	1.14×10^{-1}	0.084	3.234	222.774
BC300	4.143	0.000	15.987	1.35×10^{-2}	0.000	9.823	5.681
BC400	15.641	9.064	9.889	1.56×10^{-2}	0.008	3.983	20.144
BC500	52.525	35.745	22.130	5.01×10^{-2}	0.031	3.827	63.732
BC600	199.483	155.331	33.565	1.53×10^{-1}	0.126	3.244	226.876
BC700	340.062	188.506	61.485	2.13×10^{-1}	0.157	2.515	378.486
MC300	8.766	0.000	16.006	2.86×10^{-2}	0.000	13.071	19.154
MC400	15.212	0.000	18.368	2.96×10^{-2}	0.000	7.783	33.5943
MC500	21.061	5.162	21.389	3.77×10^{-2}	0.006	7.163	49.6047
MC600	58.703	32.323	38.805	7.21×10^{-2}	0.030	4.054	132.446
MC700	166.121	61.621	74.493	1.39×10^{-1}	0.056	3.343	397.045

[a] SSA: specific surface area. [b] MPA: micropore area. [c] ESA: external surface area. [d] TPV: total pore volume. [e] MPV: micropore volume. [f] APD: average pore diameter.

surfaces of carbonaceous adsorbent and adsorbate.[35] In contrast, these surface polar oxygen-containing functional groups were expected to form three-dimensional water clusters *via* strong H-bonding and then hinder HOCs from approaching the available adsorption sites, in turn, suppressing the adsorption of HOCs by biochars.[30] In addition, the surface polarity of biochar was also found to play an important role in controlling the adsorption of organic contaminants by π–π EDA interactions between electron-rich (π-donor) and π-acceptor sites in organic matter within the biochar.[7]

To further investigate the effects of the physicochemical properties on the adsorption capacity of biochars toward ATZ, the correlations between the OC-normalized adsorption coefficient $\log K_{oc}$ ($\log K_{oc} = \log Q_e/(C_e f_{oc})$) of ATZ at three different equilibrium concentrations and the H/C, O/C, and (O + N)/C ratios of the selected biochars are shown in Fig. 1, where S_w is the aqueous solubility of ATZ. These results indicated that the $\log K_{oc}$ values of ATZ at three different equilibrium concentrations were negatively correlated with the H/C, O/C, and (O + N)/C atomic ratios of the biochars, which suggested that aromaticity and hydrophobicity of the biochars facilitate the adsorption of ATZ. However, the polarity of biochar was not favorable for the adsorption of ATZ. Furthermore, the significant and positive correlations between the *n* values of ATZ adsorption on biochars and H/C, O/C, and (O + N)/C atomic ratios of biochars are shown in Fig. S5.† Evidently, the increase in the aromaticity and hydrophobicity of biochars was responsible for the nonlinearity in ATZ adsorption. However, the *n* values of ATZ adsorption for MC were higher than those for BC and RC, which indicated that the hydrophobic interaction played a more critical role in the adsorption of ATZ on MC.

3.3 Enhanced adsorption of ATZ by soil amended with biochars

3.3.1 Adsorption isotherms of ATZ on biochar-amended soil. The adsorption isotherms of ATZ on PS and BS amended with RC, BC, and MC are shown in Fig. 2, and the corresponding fitting parameters are listed in Table S3.† Biochar exhibited a far stronger adsorption capacity for ATZ than soil, and the addition of 2% RC700, 2% BC700, and 2% MC700 significantly enhanced the adsorption of ATZ on PS and BS, with the total adsorption amount of ATZ on biochar-amended PS and BS at $C_e = 0.5S_w$ being increased by 5.2–7.5 times and 2.3–4.2 times, respectively. This difference suggested that the enhanced adsorption of ATZ on biochar-amended soil could be partly attributed to the adsorption capacity of the original soil. The adsorption capacity of PS for ATZ was markedly weaker than that of BS, which resulted in the stronger facilitating effect of biochar for ATZ adsorption on PS. Moreover, the adsorption of ATZ on biochar-amended soil increased with the increase in the pyrolysis temperature and the addition ratio of biochars, and the sequence of enhancement was in agreement with the adsorption capacity of the original biochars (data not shown). Furthermore, the addition of RC700 was observed to have a greater facilitating effect on the adsorption of ATZ than MC700 and BC700, but did not follow the order of adsorption capacity of the corresponding biochars, which was likely due to the interaction between the biochar and soil or soil components.[14]

3.3.2 Surface-partition adsorption mechanism. Here, it is noteworthy that the *n* values of ATZ adsorption isotherms for the biochar-amended soils were much lower than those for the original soil, suggesting that the adsorption mechanism shifted from hydrophobic partition in the original soil to surface adsorption in the biochar-amended soil.[17] According to Accardi-Dey and Gschwend (2003), the partition into soil organic matter generally yielded a linear adsorption behavior, where Freundlich $n < 1$ indicates adsorption onto the biochar.[36] In addition, specific interactions between the adsorbent and adsorbate might also result in adsorption nonlinearity. Owing to the heterogeneity of the surface of the biochar and soil, the individual adsorption mechanism could not completely describe the adsorption process of the organic compounds in both soil

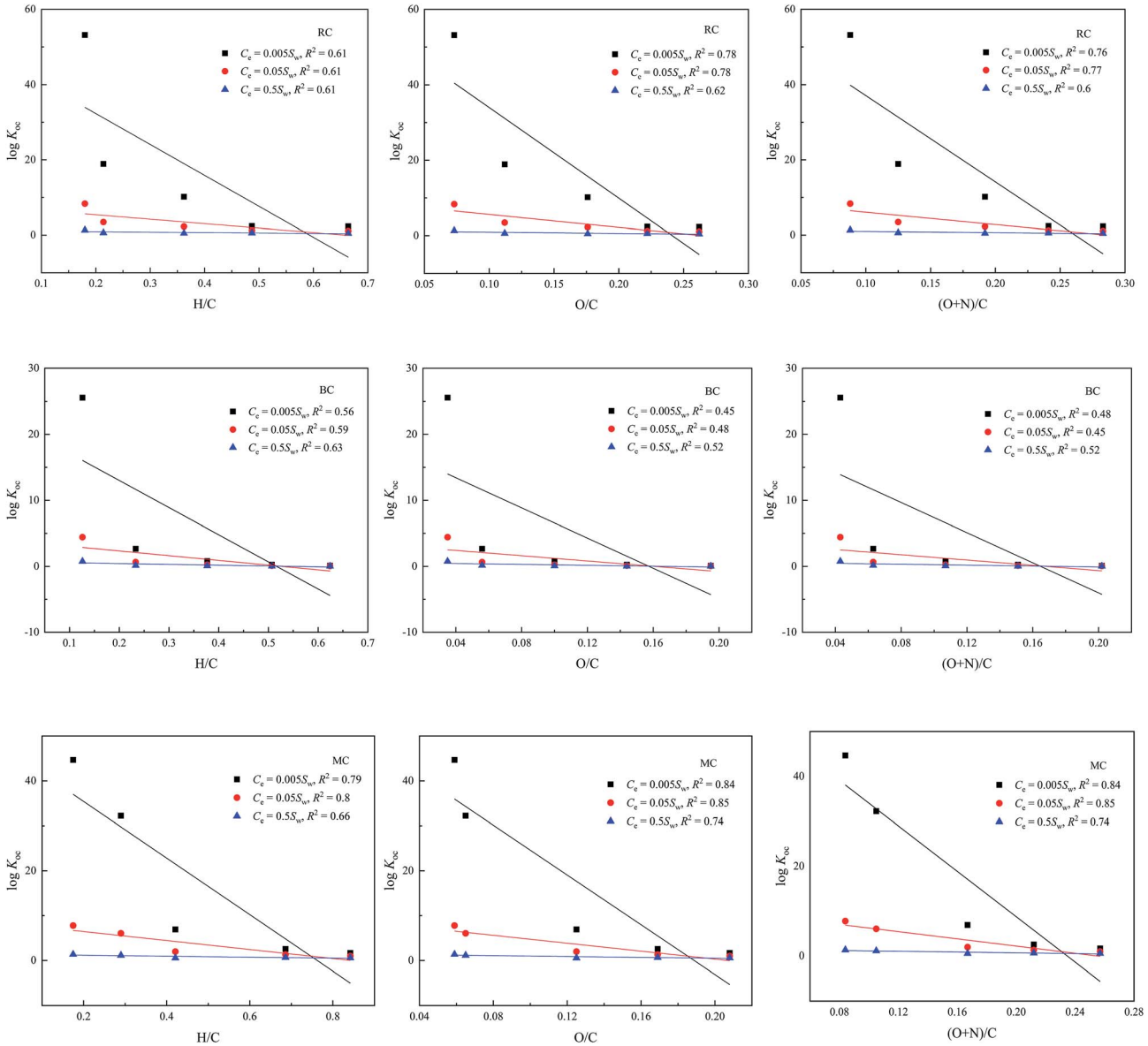

Fig. 1 Correlations between log K_{oc} (mL g^{-1}) of ATZ at three different equilibrium concentrations and H/C, O/C, and (O + N)/C atomic ratios of the selected biochars.

and biochar.[32] To better distinguish between the different adsorption mechanisms, a combined adsorption–partition model (eqn (1)) was proposed to further study the effect of biochar addition on ATZ adsorption:

$$Q_T = Q_A + Q_p = Q_A + K_p C_e \quad (1)$$

where Q_T represents the total adsorbed amount of ATZ on biochar; Q_A and Q_p are the respective contribution amounts by surface adsorption and partition adsorption, respectively; and K_p and C_e are the partition coefficient and equilibrium concentration, respectively. Linear regression was conducted in the range of $C_e/S_w > 0.2$ (the ratio of equilibrium concentration to aqueous solubility), and the surface and partition adsorption amounts of ATZ for the original soil and biochar-amended soil are indicated at $C_e = 0.5S_w$, as shown in Fig. 3. Higher Q_p values of PS and BS suggested that hydrophobic partition dominated the ATZ adsorption in the original soil. With the addition of biochar, the surface and partition adsorption amounts of ATZ on biochar-amended soil increased. However, the degree of increase in the surface adsorption amount was much higher than that of the partition adsorption amount, which could mainly be attributed to the contribution of specific adsorption of ATZ on the biochar, including the pore-filling effect and π–π EDA interaction. On the other hand, different effects of biochars and soil types on the surface adsorption and partition adsorption of ATZ on biochar-amended soil could be observed. From Fig. 3, it is evident that when compared with the addition of BC and MC, the addition of RC had a more profound effect on the increase in the surface adsorption of ATZ on PS and BS, which

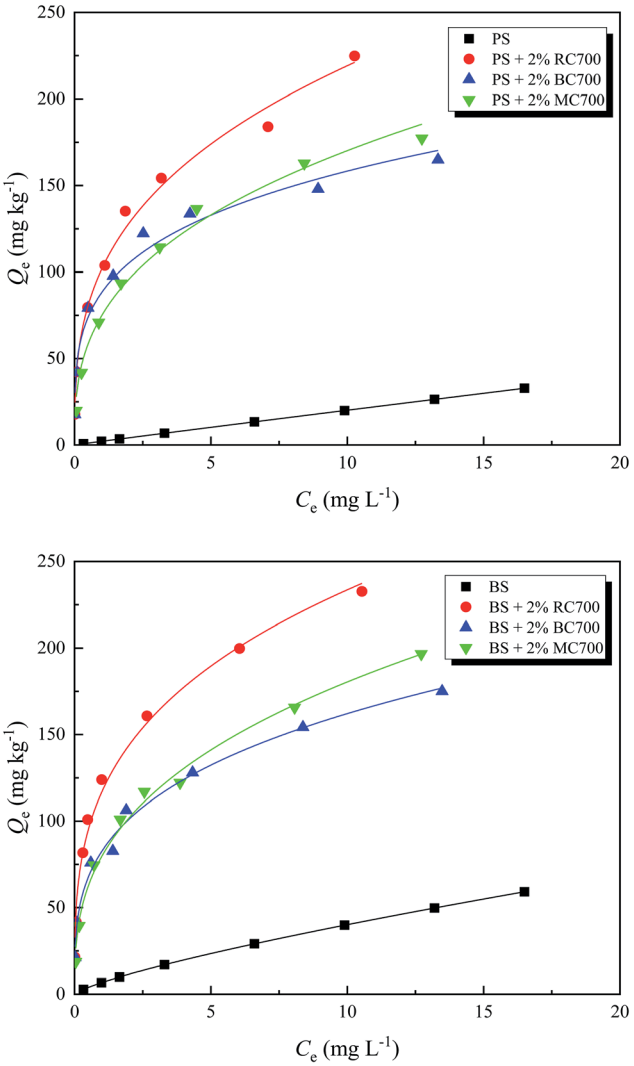

Fig. 2 Adsorption isotherms of ATZ on PS and BS amended with 2% RC, 2% BC, and 2% MC.

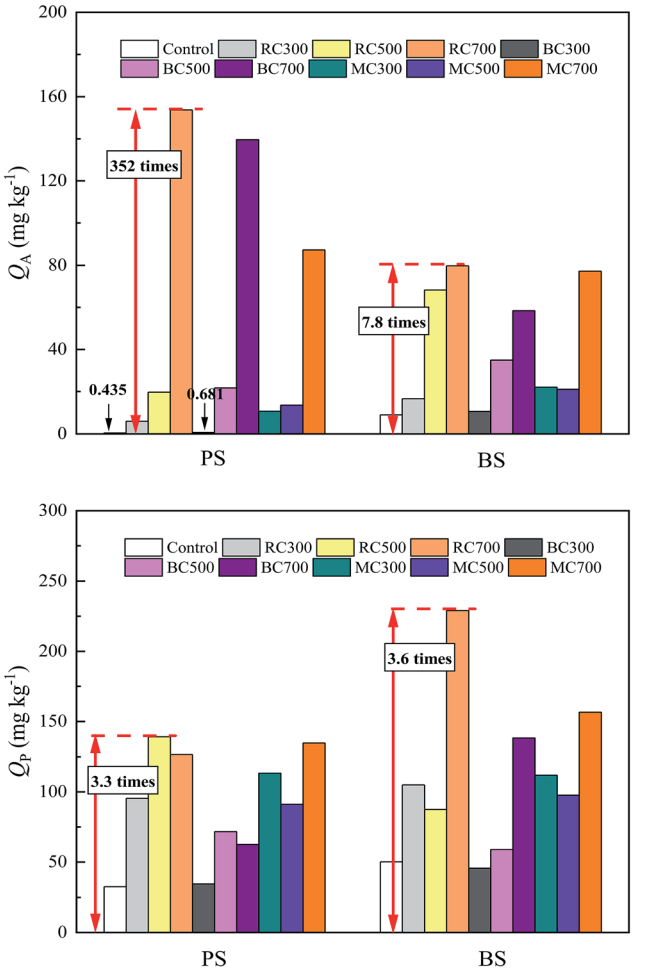

Fig. 3 Surface adsorption amount (Q_A) and partition adsorption amount (Q_P) of ATZ on soil and biochar-amended soil at $C_e = 0.5S_w$.

could be attributed to the strong π–π EDA interaction between RC and ATZ due to the higher polarity and aromaticity of RC, and this enhancement was more significant on RC-amended PS rather than RC-amended BS. By contrast, the addition of RC exerted a more positive effect on the partition adsorption of ATZ on BS than PS, which followed the same order as the partition adsorption of ATZ on the original soil.

Meanwhile, the effects of the addition ratio of biochar on the surface and partition adsorption amounts of ATZ on biochar-amended soil are shown in Fig. 4. After the addition of biochar, the partition adsorption amount of ATZ on biochar-amended soil increased with the addition ratio, whereas the surface adsorption amount of ATZ on biochar-amended soil exhibited a different changing trend due to the variation in the addition ratio of biochar. When the addition ratio of the biochar was more than 1.5%, the surface adsorption amount of ATZ for biochar-amended BS, in turn, decreased, but it still increased for biochar-amended PS, indicating that the interaction between biochar and BS might affect the surface adsorption of ATZ on biochar-amended BS. The OC content of BS was far higher than that of PS, to a certain extent, making a contribution to the partition adsorption in the mixed system. Therefore, this part of the partition adsorption could compete against the surface adsorption of biochar for adsorption sites. Moreover, the respective contributions of surface adsorption and partition adsorption toward the total adsorption of ATZ on biochar-amended soil changed with the different addition ratios of biochars.

3.3.3 Multiple nonlinear regression analysis. The adsorption of ATZ after the addition of biochar to soil was determined by the aromaticity, polarity, and hydrophobicity of the added biochar, in addition to its SSA and OC content.[12,14,37] For instance, Spokas *et al.* reported that the high adsorption of ATZ and acetochlor was observed in sandy loam soil amended with 5% (w/w) sawdust biochar,[37] which was ascribed to the high OC content and SSA of biochar; Zhang *et al.* found that biochar amendment increased the thiacloprid adsorption in soil, which was associated with an increase in OC and a decrease in H/C;[14] Jin *et al.* suggested that the enhanced adsorption capacity of biochar-amended soil for ATZ and imidacloprid could be attributed to the increased surface area of the biochar as well as

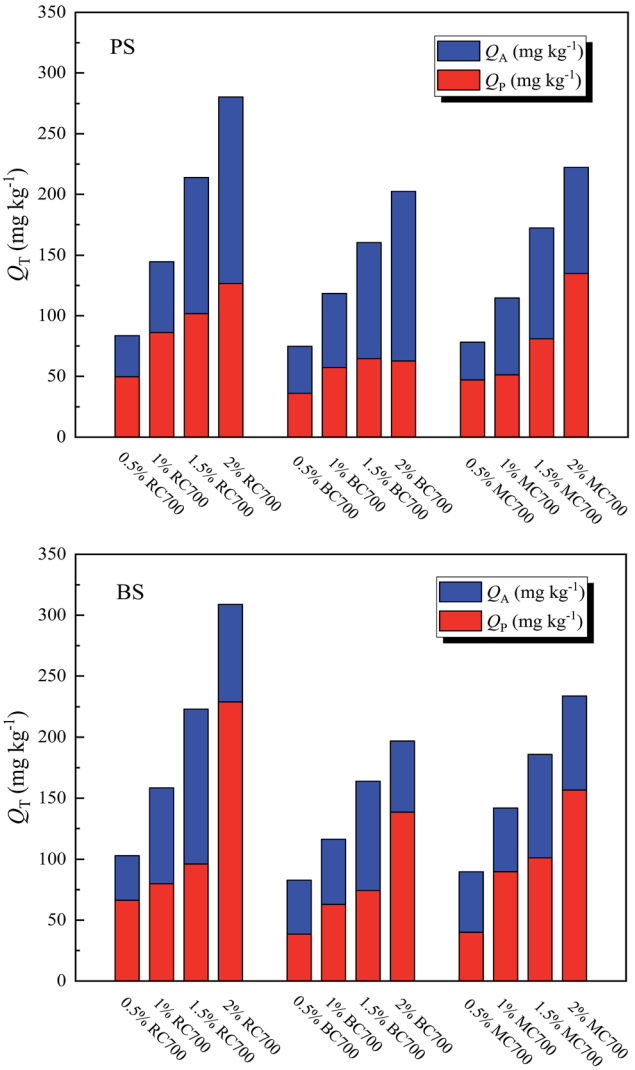

Fig. 4 Effect of addition ratio of biochar on Q_A and Q_P of ATZ on biochar-amended soils.

the decreased hydrophobicity.[12] In addition, another study demonstrated that the dissolved OC and clay minerals in soil had a significant effect on reducing the efficiency of phenanthrene and pyrene adsorption by the biochars.[34] However, the quantitative evaluation for the relationship between the adsorption capacity of biochar-amended soil and the corresponding properties of the added biochar was hardly reported in earlier studies. To clearly reveal the relationship between the surface adsorption and partition adsorption of ATZ on biochar-amended soils with the biochar properties and to further evaluate the effects of biochar properties on the adsorption behavior of biochar-amended soil, a second-order polynomial equation (eqn (2)–(5)) was, therefore, determined *via* using multiple nonlinear regression analysis; three-dimensional surface plots of the interactive effects of the studied biochar properties on the adsorption behavior of ATZ on biochar-amended soil are shown in Fig. 5.

$$Y_{A\text{-}PS} = +399.1 + 736.8x_1^2 + 2875.7x_2^2 - 951.6x_1 - 1116.2x_2 - 0.487x_5;\ (R^2 = 0.903) \quad (2)$$

$$Y_{P\text{-}PS} = -190.5 - 394x_3^2 - 0.043x_4^2 + 616.1x_3 + 4.5x_4;\ (R^2 = 0.762) \quad (3)$$

$$Y_{A\text{-}BS} = +324.9 + 625.9x_1^2 + 964x_2^2 - 875.5x_1 - 258.2x_2 - 0.75x_5;\ (R^2 = 0.943) \quad (4)$$

$$Y_{P\text{-}BS} = +407.8 + 1038.7x_1^2 - 1206.5x_1 - 0.17x_5;\ (R^2 = 0.753) \quad (5)$$

where x_1, x_2, x_3, x_4, and x_5 are the coded values for the H/C ratio, (O + N)/C ratio, OC content, ash content, and SSA, respectively. $Y_{A\text{-}PS}$, $Y_{P\text{-}PS}$, $Y_{A\text{-}BS}$, and $Y_{P\text{-}BS}$ represent the surface adsorption amounts and partition adsorption amounts of ATZ on biochar-amended PS and BS, respectively, at $C_e = 0.5S_w$. First, the surface adsorption amounts of ATZ on biochar-amended PS and biochar-amended BS could be expressed as a function of H/C ratio, (O + N)/C ratio, and SSA of the added biochar, and the partition adsorption amount of ATZ on biochar-amended PS could be expressed as a function of OC and ash content; on the contrary, the partition adsorption amount of ATZ on biochar-amended BS could be expressed as a function of H/C ratio and SSA of the added biochar, as shown in eqn (2)–(5). Moreover, the multiple nonlinear regression analysis suggested the linear dependence of H/C ratio, (O + N)/C ratio, and SSA on the surface adsorption capacities of biochar-amended PS and biochar-amended BS; further, it suggested the linear dependence of OC and ash contents on the partition adsorption capacity of biochar-amended PS and the linear dependence of H/C ratio and SSA on the partition adsorption capacity of biochar-amended BS.

In addition, from Fig. 5a, it is obvious that the surface adsorption amount of ATZ on biochar-amended PS significantly decreased with the increase in the H/C ratio of biochar, but slightly decreased with the increase in the (O + N)/C ratio. Furthermore, the partition adsorption amount of ATZ on biochar-amended PS considerably increased with the increasing ash content of the biochar, but hardly changed with increasing OC content (Fig. 5b). This result indicated that high aromaticity of biochar facilitated the surface adsorption of ATZ on biochar-amended soil, while the high ash content of biochar was favorable toward partition adsorption. Similarly, the surface adsorption amount of ATZ on biochar-amended BS also exhibited a significant decrease with an increase in the H/C ratio of biochar (Fig. 5c), suggesting the positive effect of biochar aromaticity on the surface adsorption of ATZ on biochar-amended BS. On the contrary, the partition adsorption amount of ATZ on biochar-amended BS initially decreased and then slightly increased with the increasing H/C ratio of biochar, but slightly decreased with increasing SSA (Fig. 5d). This difference demonstrated that the effect of biochar aromaticity on the partition adsorption of biochar-amended BS had major significance. According to the above analysis, it seemed reasonable to assume that the adsorption behavior of ATZ on

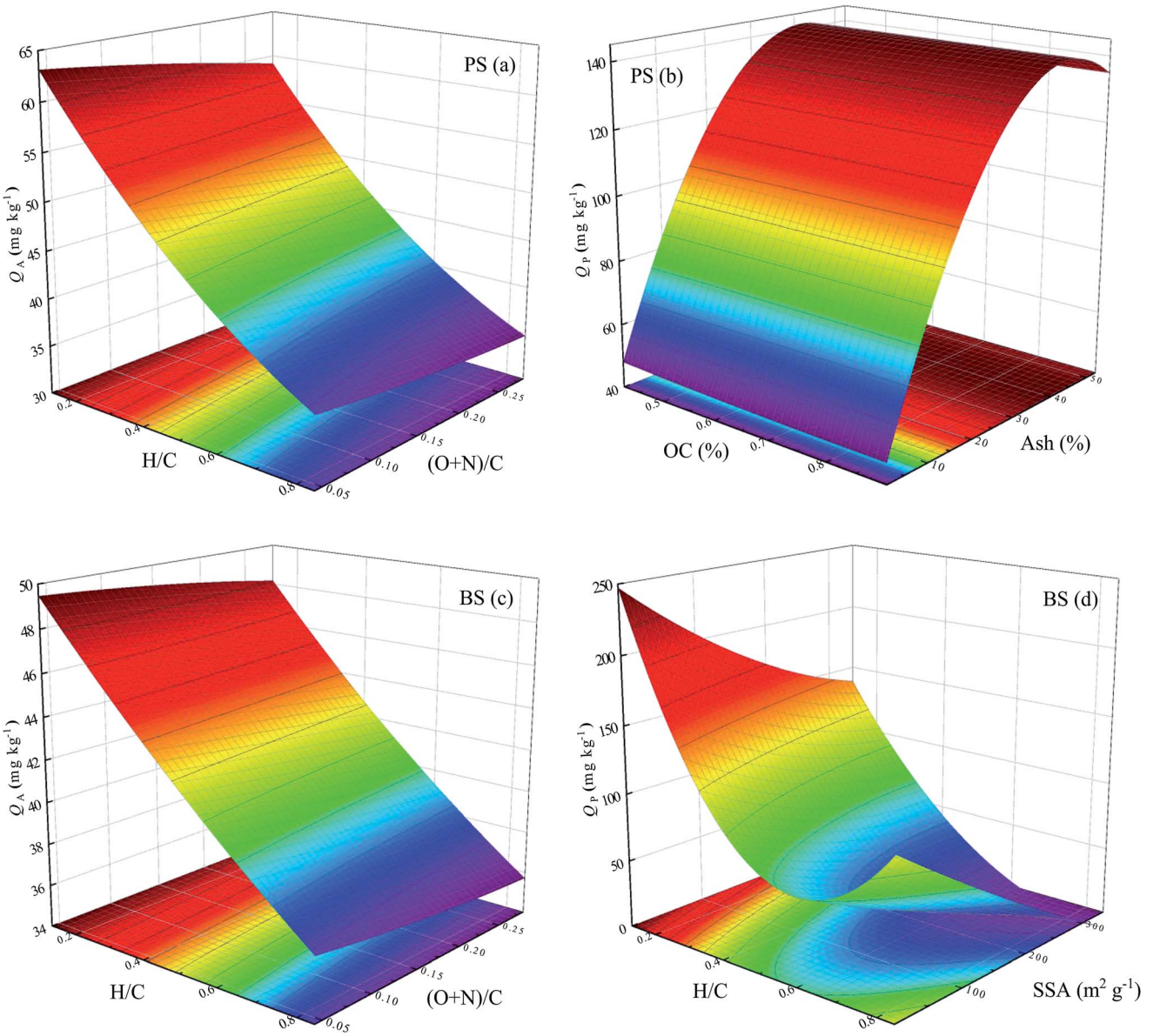

Fig. 5 Three-dimensional surface plots of the interactive effects of studied biochar properties on the adsorption behavior of ATZ on biochar-amended soils. (a), (b), (c), and (d) represent the interactive effects of H/C and (O + N)/C ratios of biochar on the surface adsorption of ATZ onto biochar-amended PS, interactive effects of OC and ash contents of biochar on the partition adsorption of ATZ onto biochar-amended PS, interactive effects of H/C and (O + N)/C ratios of biochar on the surface adsorption of ATZ onto biochar-amended BS, and interactive effects of H/C ratio and SSA of biochar on the partition adsorption of ATZ onto biochar-amended BS, respectively.

biochar-amended soil could be simultaneously influenced by multiple properties of the added biochars.

3.4 Evidence for biochar–soil interaction in affecting the adsorption of ATZ in biochar-amended soils

Although the adsorption of ATZ on biochar-amended soil depended on the combination of adsorption of soil and biochar, it has been widely acknowledged that the interaction between biochar and soil/soil constituents, referring to the adsorption of dissolved OC of soil by biochar, and adsorption of authigenic organic matter of biochar by soil minerals, and insertion and attachment of minerals on biochar surfaces, and electron transfer functionality of biochars after interacting with soil minerals, might induce changes in the adsorption capacity of organic compounds.[38–40] To precisely examine whether and how the interaction would affect the adsorption of ATZ on biochar-amended soils, the real adsorption amounts of ATZ on PS and BS amended with 2% RC, 2% BC, and 2% MC were compared with the predicted adsorption amounts at $C_e/S_w < 1$, which were calculated based on the following equation:

$$Q_{predict} = f_{soil}K_{f,soil}C_e^{n,soil} + f_{biochar}K_{f,biochar}C_e^{n,biochar} \quad (6)$$

where $Q_{predict}$ is the predicted adsorption amount of ATZ on biochar-amended soil; f_{soil} and $f_{biochar}$ are the mass fractions of

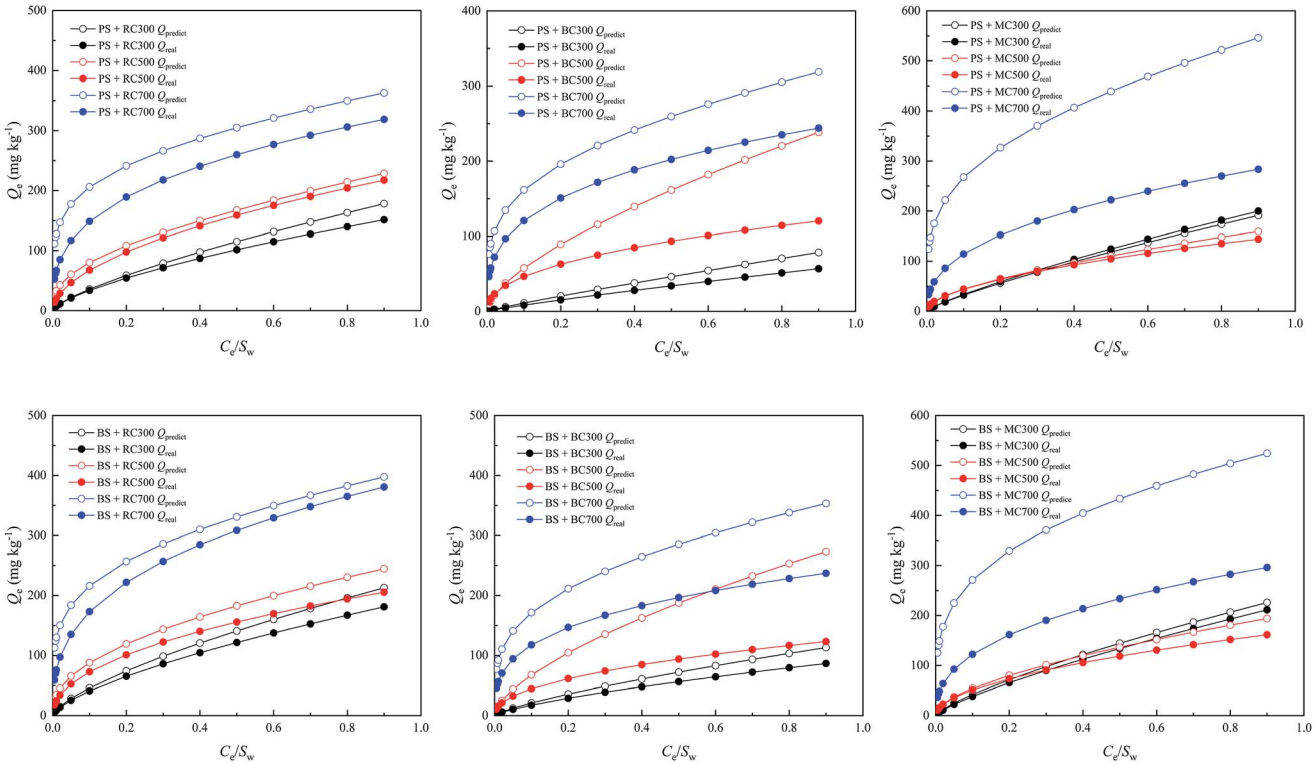

Fig. 6 Comparison between the predicted adsorption amounts ($Q_{predict}$) and real adsorption amounts (Q_{real}) of ATZ on PS and BS amended with 2% RC, 2% BC, and 2% MC.

soil and biochar in the biochar-amended soil, respectively; $K_{f,soil}$, $C_e^{n,soil}$, $K_{f,biochar}$, and $C_e^{n,biochar}$ are the Freundlich model parameters of ATZ in soil and biochar, respectively. The comparison between the predicted and real adsorption amounts of ATZ on biochar-amended soil is shown in Fig. 6.

Apparently, the real adsorption amounts of ATZ on biochar-amended soil were far lower than the predicted adsorption amounts; moreover, the attenuation effect was more obvious with the increase in the ATZ equilibrium concentration in an aqueous solution. This further proved that biochar would interact with the soil/soil components to influence the adsorption capacity of biochar-amended soil for ATZ. In particular, for the soil amended with high-temperature biochar (700 °C), the differences between the real and predicted adsorption amounts of ATZ on MC-amended soil were much greater than those on BC- and RC-amended soils, which indicated that the interaction of MC with soil exceeded those of RC and BC. This was because MC has higher ash content than BC and RC, which was detrimental toward adsorption due to the blocked and inaccessible organic adsorption sites in the original biochar.

Interestingly, the real adsorption amounts of ATZ on PS and BS amended with 2% RC300, 2% BC300, and 2% MC300 were more approximate to their predicted adsorption amounts, respectively, when compared with those of ATZ on PS and BS amended with 2% RC700, 2% BC700, and 2% MC700. It was based on traditional acceptance, which suggested that dissolved organic matter and native adsorbate in soils decreased the adsorption of ATZ on biochar by competing for or blocking the surface adsorption sites of biochar.[13,39,41] However, new evidence has revealed the potential mechanism in which organic matter in biochar might compensate the role of soil organic matter in the competition for adsorption sites with a decrease in biochar pyrolysis temperatures, thereby narrowing the difference between the real and predicted adsorption amounts of ATZ. In addition to the effect of organic matter on ATZ adsorption, soil minerals, a major soil component, could prevent the exposure of carbon and oxygen by providing physical isolation and then suppress the formation of O-containing functional groups on the biochar surface, which was not favorable for the adsorption of ATZ.[3,7]

4. Conclusions

In this study, the adsorption of ATZ on BS and PS was considerably enhanced due to the amendment of different types of biochars; moreover, this enhancement was dependent on the pyrolysis temperature, addition ratio, and physicochemical properties of biochar. In addition, biochar-amended soils exhibited stronger nonlinearity adsorption when compared with original soils. The surface and partition adsorption amounts of ATZ on biochar-amended soil increased with the amendment of biochar. However, the degree of increase of the surface adsorption amount was much higher than that of the partition adsorption amount. The multiple nonlinear regression analysis, combined with the three-dimensional surface plots of the interactive effects of the studied biochar properties

on the adsorption behavior of ATZ on biochar-amended soil indicated that the adsorption behavior of ATZ on biochar-amended soil could be simultaneously influenced by the amended multiple biochar properties. In addition, the interaction between the different biochar properties might affect the adsorption of ATZ in biochar-amended soil mixtures. The real adsorption amounts of ATZ on biochar-amended soils were far lower than the predicted adsorption amounts, suggesting the interaction between biochar and soil/soil components, including dissolved organic matter and soil minerals.

Conflicts of interest

There are no conflicts to declare.

Acknowledgements

This study was financially supported by the National Natural Science Foundation of China (21577124) and the National Key Research and Development Program of China (2017YFA0207002).

References

1 C. Peiris, S. R. Gunatilake, T. E. Mlsna, D. Mohan and M. Vithanage, *Bioresour. Technol.*, 2017, **246**, 150–159.
2 M. Safaei Khorram, Q. Zhang, D. L. Lin, Y. Zheng, H. Fang and Y. L. Yu, *J. Environ. Sci.*, 2016, **44**, 269–279.
3 F. Yang, L. Zhao, B. Gao, X. X. Xu and X. D. Cao, *Environ. Sci. Technol.*, 2016, **50**, 2264–2271.
4 M. Kah, G. Sigmund, F. Xiao and T. Hofmann, *Water Res.*, 2017, **124**, 673–692.
5 D. Y. Xu, Y. Zhao, K. Sun, B. Gao, Z. Y. Wang, J. Jin, Z. Y. Zhang, S. F. Wang, Y. Yan, X. T. Liu and F. C. Wu, *Chemosphere*, 2014, **111**, 320–326.
6 W. J. Liu, H. Jiang and H. Q. Yu, *Chem. Rev.*, 2015, **115**, 12251–12285.
7 K. Sun, M. J. Kang, Z. Y. Zhang, J. Jin, Z. Y. Wang, Z. Z. Pan, D. Y. Xu, F. C. Wu and B. S. Xing, *Environ. Sci. Technol.*, 2013, **47**, 11473–11481.
8 Y. Y. Zhou, X. C. Liu, Y. J. Xiang, P. Wang, J. C. Zhang, F. F. Zhang, J. H. Wei, L. Luo, M. Lei and L. Tang, *Bioresour. Technol.*, 2017, **245**, 266–273.
9 F. R. Oliveira, A. K. Patel, D. P. Jaisi, S. Adhikari, H. Lu and S. K. Khanal, *Bioresour. Technol.*, 2017, **246**, 110–122.
10 Y. Y. Zhou, Y. Z. He, Y. J. Xiang, S. J. Meng, X. C. Liu, J. F. Yu, J. Yang, J. C. Zhang, P. F. Qin and L. Luo, *Sci. Total Environ.*, 2019, **646**, 29–36.
11 M. Kah, G. Sigmund, P. L. Manga Chavez, L. Bielská and T. Hofmann, *PeerJ*, 2018, **6**, e4996.
12 J. Jin, M. J. Kang, K. Sun, Z. Z. Pan, F. C. Wu and B. S. Xing, *Sci. Total Environ.*, 2016, **550**, 504–513.
13 X. H. Ren, H. W. Sun, F. Wang, P. Zhang and H. K. Zhu, *Environ. Pollut.*, 2018, **242**, 1880–1886.
14 P. Zhang, H. W. Sun, L. J. Min and C. Ren, *Environ. Pollut.*, 2018, **236**, 158–167.
15 F. Lian and B. S. Xing, *Environ. Sci. Technol.*, 2017, **51**, 13517–13532.
16 K. B. Delwiche, J. Lehmann and M. T. Walter, *Chemosphere*, 2014, **95**, 346–352.
17 A. Dechene, I. Rosendahl, V. Laabs and W. Amelung, *Chemosphere*, 2014, **109**, 180–186.
18 Y. P. Qiu, M. W. Wu, J. Jiang, L. Li and G. Daniel Sheng, *Chemosphere*, 2013, **93**, 69–74.
19 K. G. I. D. Kumari, P. Moldrup, M. Paradelo and L. W. de Jonge, *Water, Air, Soil Pollut.*, 2014, **225**, 2105.
20 G. Cornelissen, Ö. Gustafsson, T. D. Bucheli, M. T. O. Jonker, A. A. Koelmans and P. C. M. van Noort, *Environ. Sci. Technol.*, 2005, **39**, 6881–6895.
21 B. L. Chen and M. X. Yuan, *J. Soils Sediments*, 2011, **11**, 62–71.
22 M. S. Khorram, A. K. Sarmah and Y. Yu, *Water, Air, Soil Pollut.*, 2018, **229**, 60.
23 F. Yang, W. Zhang, J. M. Li, S. Y. Wang, Y. Tao, Y. F. Wang and Y. Zhang, *Chemosphere*, 2017, **189**, 507–516.
24 X. Y. Yu, G. G. Ying and R. S. Kookana, *J. Agric. Food Chem.*, 2006, **54**, 8545–8550.
25 P. Zhang, H. W. Sun, C. Ren, L. J. Min and H. M. Zhang, *Environ. Pollut.*, 2018, **234**, 812–820.
26 C. Anyika, Z. Abdul Majid, Z. Ibrahim, M. P. Zakaria and A. Yahya, *Environ. Sci. Pollut. Res.*, 2015, **22**, 3314–3341.
27 J. F. Li, J. S. Li, H. P. Dong, S. S. Yang, Y. M. Li and J. X. Zhong, *J. Agric. Food Chem.*, 2015, **63**, 5740–5746.
28 S. Y. Wei, M. B. Zhu, J. Z. Song and P. A. Peng, *BioResources*, 2017, **12**, 3316–3330.
29 B. P. Koch and T. Dittmar, *Rapid Commun. Mass Spectrom.*, 2006, **20**, 926–932.
30 I. J. Schreiter, W. Schmidt and C. Schüth, *Chemosphere*, 2018, **203**, 34–43.
31 A. Mandal, N. Singh and T. J. Purakayastha, *Sci. Total Environ.*, 2017, **577**, 376–385.
32 H. Deng, D. Feng, J. X. He, F. Z. Li, H. M. Yu and C. J. Ge, *Ecol. Eng.*, 2017, **99**, 381–390.
33 J. Jin, K. Sun, Z. Y. Wang, L. F. Han, P. Du, X. K. Wang and B. S. Xing, *Sci. Total Environ.*, 2017, **598**, 789–796.
34 A. Zielińska and P. Oleszczuk, *Environ. Sci. Pollut. Res.*, 2016, **23**, 21822–21832.
35 E. Rosales, J. Meijide, M. Pazos and M. A. Sanromán, *Bioresour. Technol.*, 2017, **246**, 176–192.
36 A. Accardi-Dey and P. M. Gschwend, *Environ. Sci. Technol.*, 2003, **37**, 99–106.
37 K. A. Spokas, W. C. Koskinen, J. M. Baker and D. C. Reicosky, *Chemosphere*, 2009, **77**, 574–581.
38 J. Jin, K. Sun, W. Liu, S. W. Li, X. Q. Peng, Y. Yang, L. F. Han, Z. W. Du and X. K. Wang, *Environ. Pollut.*, 2018, **236**, 745–753.
39 X. H. Ren, X. J. Yuan and H. W. Sun, *Environ. Sci. Pollut. Res.*, 2018, **25**, 81–90.
40 Z. D. Zhao and W. J. Zhou, *Environ. Pollut.*, 2019, **245**, 208–217.
41 S. M. Martin, R. S. Kookana, L. Van Zwieten and E. Krull, *J. Hazard. Mater.*, 2012, **231–232**, 70–78.